On High-Order Upwind Methods for Advection

H. T. Huynh

NASA Glenn Research Center, MS 5-11, Cleveland, OH 44135, USA.

Email: huynh@grc.nasa.gov

Abstract. In the fourth installment of the celebrated series of five papers entitled "Towards the ultimate conservative difference scheme", Van Leer (1977) introduced five schemes for advection, the first three are piecewise linear, and the last two, piecewise parabolic. Among the five, scheme I, which is the least accurate, extends with relative ease to systems of equations in multiple dimensions. As a result, it became the most popular and is widely known as the MUSCL scheme (monotone upstream-centered schemes for conservation laws). Schemes III and V have the same accuracy, are the most accurate, and are closely related to current high-order methods. Scheme III uses a piecewise linear approximation that is discontinuous across cells, and can be considered as a precursor of the discontinuous Galerkin methods. Scheme V employs a piecewise quadratic approximation that is, as opposed to the case of scheme III, continuous across cells. This method is the basis for the on-going "active flux scheme" developed by Roe and collaborators. Here, schemes III and V are shown to be equivalent in the sense that they yield identical (reconstructed) solutions, provided the initial condition for scheme III is defined from that of scheme V in a manner dependent on the CFL number. This equivalence is counter intuitive since it is generally believed that piecewise linear and piecewise parabolic methods cannot produce the same solutions due to their different degrees of approximation. The finding also shows a key connection between the approaches of discontinuous and continuous polynomial approximations. In addition to the discussed equivalence, a framework using both projection and interpolation that extends schemes III and V into a single family of high-order schemes is introduced. For these high-order extensions, it is demonstrated via Fourier analysis that schemes with the same number of degrees of freedom K per cell, in spite of the different piecewise polynomial degrees, share the same sets of eigenvalues and thus, have the same stability and accuracy. Moreover, these schemes are accurate to order $2K - 1$, which is higher than the expected order of K.

Keywords. High-order methods, upwind schemes, advection equation.

1. Introduction

In the field of Computational Fluid Dynamics (CFD), second-order methods are currently popular. However, results by these methods for turbulent and unsteady flows, which play a critical role in industrial applications, are not reliable. Leading researchers generally agree that high-order (third or higher) methods are promising for such problems. The need to develop, test, and employ high-order methods has attracted the interest of many computational fluid dynamicists as evidenced by the numerous papers at conferences, the recent series of International Workshop on High-Order CFD Methods (1st-4th), and the ongoing TILDA project (Towards Industrial LES and DNS for Aeronautics) supported by the European Union.

Popular high-order methods are typically piecewise polynomial, i.e., the solution is approximated by a polynomial in each cell. The function formed by these polynomials for all cells can be either continuous or discontinuous across cell interfaces. Examples of the former are the finite-element methods (Hughes 1987, Johnson 1987) and recently the active flux scheme (Eymann and Roe 2013). Examples of the latter are the discontinuous Galerkin (Cockburn, Karniadakis, and Shu 2000, Hesthaven and Warburton 2008), spectral

volume (Wang et al. 2004), spectral difference (Liu et al., 2006) and, more recently, the flux reconstruction method (Huynh 2007, 2009, Huynh, Wang, and Vincent, 2014), which provides a unifying framework for schemes of discontinuous type.

Concerning basic algorithm developments, the advection equation serves as a fertile ground to construct and test numerical schemes. A method devised for advection must then be extended to systems of equations in multiple dimensions, which is often not a trivial task. In fact, even methods in the same family, such as Van Leer's schemes discussed below, may encounter different levels of difficulty in their extensions.

In the fourth installment of the celebrated series of five papers entitled "Towards the ultimate conservative difference scheme", Van Leer (1977) introduced five schemes for advection, the first three are piecewise linear, and the last two, piecewise parabolic. Among the five, scheme I, which is the least accurate, extends with relative ease to systems of equations in multiple dimensions. As a result, it became the most popular and is widely known as the MUSCL scheme (monotone upstream-centered schemes for conservation laws). Scheme IV, which is the parabolic counterpart of scheme I, also extends but is more involved. This extension was carried out by Colella and Woodward (1984) and called PPM (piecewise parabolic method), but it is not nearly as popular as the piecewise linear MUSCL scheme. Schemes II, III, and V differ from schemes I and IV in that for each cell, they carry along not only the cell average value, but also an additional quantity such as the interface value(s) or the slope. After nearly three decades, Van Leer lamented about these methods in (Van Leer and Nomura 2005): "When trying to extend these schemes beyond advection, viz., to a nonlinear hyperbolic system like the Euler equations, the first author ran into insuperable difficulties because the exact shift operator no longer applies, and he abandoned the idea".

The difficulty of extending scheme III to systems of equations was overcome by the author in (Huynh 2006). The resulting method is called the upwind moment scheme. The approach was further analyzed and applied to hyperbolic-relaxation equations for continuum-transition flows in (Suzuki and Van Leer 2007, Suzuki 2008, Khieu, Suzuki, and Van Leer 2009). As briefly discussed in (Huynh 2007), the moment scheme can be extended to arbitrary order. Such an extension was independently obtained by Lo and was studied in combination with Van Leer's recovery scheme for diffusion in his PhD dissertation (2011). Extensions of the moment scheme to arbitrary order in multiple dimensions were carried out in (Huynh 2013); it was shown that extensions to high-order in two spatial dimensions encounter the drawback of a restrictive CFL condition, as opposed to the case of systems of equations in one spatial dimension where the CFL condition is 1 for all polynomial degrees. For scheme V, the difficulty of extension is being tackled by Roe and collaborators in the "active flux scheme" (Eymann and Roe 2013, Fan and Roe 2015).

In this paper, schemes III and V are shown to be equivalent in the sense that they yield identical solutions, provided the initial condition for scheme III is defined or extracted from that of scheme V in a manner dependent on the CFL number. Since the solution is piecewise linear for scheme III and piecewise parabolic for scheme V, they are identical in that they satisfy the same extraction criteria employed to define the initial data for scheme III. This equivalence is counter intuitive since it is generally believed that piecewise linear and piecewise parabolic methods cannot produce the same solutions due to their different degrees of approximation. The finding also shows a key connection between the approaches of discontinuous and continuous polynomial approximations, therefore, could help bridge the gap between them. (There has been much debate concerning the trade-offs between continuous and discontinuous approaches.) In addition to the discussed equivalence, a framework employing both projection and interpolation that extends schemes III and V into a single family of high-order schemes is introduced. For these high-order extensions, it is demonstrated via Fourier analysis that schemes with the same number of degrees of freedom, say K, per cell have the following remarkable property: in spite of the different polynomial degrees, they share the same sets of eigenvalues and thus, have the same stability and accuracy. Moreover, these schemes are accurate to order $2K-1$, which is higher than the expected order of K, i.e., they are super accurate or super convergent. For schemes with the same K, the finding concerning the same sets of eigenvalues suggests a possible equivalence in a manner similar to the equivalence between schemes III and V.

Due to the basic nature of the topic and in the hope of attracting the interest of researchers not familiar with these methods, this paper is written in a self-contained manner. It is organized as follows. Section 2 reviews the advection equation and preliminaries. Section 3 discusses Van Leer's schemes III and V as well as a key part of this paper: the statement and proof of the equivalence of these two schemes. A framework that extends schemes III and V into a single family of high-order schemes is introduced in Section 4. Fourier analyses are presented in Section 5. Conclusions and discussions can be found in Section 6.

2 Advection Equation and Preliminaries

Consider the scalar advection equation

$$u_t + au_x = 0 \tag{2.1}$$

with initial condition at $t = 0$,

$$u(x, 0) = u_0(x) \tag{2.2}$$

where t is time, x space, and $a \geq 0$ the advection speed. By assuming that u_0 is periodic or of compact support, boundary conditions are trivial and therefore omitted. The exact solution at time t is obtained by shifting the data curve to the right a distance at,

$$u_{\text{exact}}(x, t) = u_0(x - at). \tag{2.3}$$

Next, Van Leer's approach, which extends Godunov's first-order upwind method (1959), is reviewed.

2.1 Discretization

For simplicity but not necessity, assume the mesh is uniform with mesh width Δx. Let the domain of calculation be divided into non-overlapping cells (or elements) $E_j = \left[x_{j-1/2},\ x_{j+1/2}\right]$ with cell centers $x_j = j\Delta x$ and interfaces $x_{j+1/2} = (j + 1/2)\Delta x$. For each E_j, as is standard when dealing with the Legendre polynomials, let the local coordinate ξ on $I = [-1, 1]$ be defined by

$$\xi = \frac{x - x_j}{\frac{1}{2}\Delta x}. \tag{2.4}$$

Conversely, the global coordinate for E_j be given by

$$x(\xi) = x_j + \frac{1}{2}\xi\Delta x. \tag{2.5}$$

Denote the time step by Δt and the CFL number by

$$\sigma = \frac{a\Delta t}{\Delta x}. \tag{2.6}$$

Then, since $a \geq 0$, the CFL condition is the requirement that

$$0 \leq \sigma \leq 1. \tag{2.7}$$

That is, in one time step, the wave advects a distance no more than one cell width.

With a fixed t^n, the solution $u(x,t^n)$ is approximated on each cell E_j by a polynomial in x denoted by $w_j^n(x) = w_j(x,t^n)$. The function formed by w_j^n (on E_j) as j varies is denoted by w^n,

$$w^n(x) = w(x,t^n) = \{w_j^n(x)\},$$

which can be continuous or discontinuous across cell interfaces.

For simplicity of notation, when there is no confusion, the superscript n for the data at time t^n is omitted, e.g., w_j^n is abbreviated to w_j, and w^n to w. The superscript $n+1$ for the solution time level, however, is always retained.

At time t^n, the function $w_j(x)$ in the global coordinate x on E_j results in $w_j(x(\xi))$ in the local coordinate ξ on $I = [-1,1]$ via (2.5). Following the common practice in the chain rule $\frac{dy}{dx} = \frac{dy}{du}\,\frac{du}{dx}$, the same notation w_j is employed for both $w_j(\xi)$ and $w_j(x)$. Loosely put,

$$w_j(\xi) = w_j(x(\xi)). \tag{2.8}$$

Generally, it is clear which coordinate is being employed, e.g., the right interface value $w_j(x_{j+1/2})$ (global) is identical to $w_j(1)$ (local).

2.2 Cell Average Solution

Given the piecewise polynomial data $w(x) = \{w_j(x)\}$ at time t^n, the corresponding solution at time t^{n+1} can be obtained by shifting the data curve to the right a distance $a\Delta t$. Denote this function by v,

$$v(x) = w(x - a\Delta t). \tag{2.9}$$

On E_j, the local coordinate for $x - a\Delta t$ is, by (2.4) and (2.6),

$$\frac{x - a\Delta t - x_j}{\frac{1}{2}\Delta x} = \xi - 2\sigma.$$

Thus, after one time step Δt, in the local coordinate, the wave travels a distance 2σ and, on E_j,

$$v_j(\xi) = \begin{cases} w_{j-1}(\xi - 2\sigma + 2), & \text{if } -1 \le \xi < -1 + 2\sigma \\ w_j(\xi - 2\sigma), & \text{if } -1 + 2\sigma \le \xi \le 1 \end{cases}. \tag{2.10}$$

The value of v_j at $\xi = -1 + 2\sigma$ does not play any role since the solutions below are obtained by integration.

The cell average solution on E_j at time t^{n+1} is denoted by $u_{j,0}^{n+1}$ and given by

$$u_{j,0}^{n+1} = \frac{1}{2}\left(\int_{1-2\sigma}^{1} w_{j-1}(\eta)\ d\eta + \int_{-1}^{1-2\sigma} w_j(\eta)\ d\eta\right) \tag{2.11}$$

or

$$u_{j,0}^{n+1} = \frac{1}{2}\left(\int_{-1}^{-1+2\sigma} w_{j-1}(\xi - 2\sigma + 2)\ d\xi + \int_{-1+2\sigma}^{1} w_j(\xi - 2\sigma)\ d\xi \right) \tag{2.12}$$

The notation $u_{j,0}^{n+1}$ will be generalized to $u_{j,k}^{n+1}$ involving the Legendre polynomial of degree k later.

3 Third-Order Accurate Schemes for Advection

Schemes III and V are reviewed and their equivalence is established in this section.

3.1 Van Leer's Scheme III

The key idea is to obtain the solution by projecting onto the space of piecewise linear functions. At time t^n, the solution $u(x, t^n)$ is approximated on each cell E_j by a linear function w_j; in the local coordinate,

$$w_j(\xi) = u_{j,0} + u_{j,1}\,\xi \tag{3.1}$$

where $u_{j,0}$ represents the cell average of u,

$$u_{j,0} \approx \frac{1}{2}\int_{-1}^{1} u\left(x_j + \tfrac{1}{2}\xi\Delta x, t^n\right) d\xi, \tag{3.2}$$

and $u_{j,1}$ represents the first moment,

$$u_{j,1} \approx \frac{3}{2}\int_{-1}^{1} \xi\, u\left(x_j + \tfrac{1}{2}\xi\Delta x, t^n\right) d\xi. \tag{3.3}$$

Recall that the factor $\frac{3}{2}$ is a consequence of the square of the L_2 norm of ξ: $\|\xi\|^2 = \int_{-1}^{1} \xi^2\, d\xi = \frac{2}{3}$. (See also (4.6) later.)

Note that, by (3.1), $w_j(1) - w_j(-1) = 2u_{j,1}$. By considering Δx as unit length, $w_j(1) - w_j(-1)$ is a scaled slope quantity; thus, $u_{j,1}$ is a scaled half slope and, at the right interface, $w_j(1) = u_{j,0} + u_{j,1}$.

The piecewise linear function $w(x, t^n)$ can be and usually is discontinuous across the interfaces. Let the projection of the initial data onto the space of piecewise linear functions be carried out by (3.2) and (3.3) with t^n replaced by t^0 (more on this later), and let the result be denoted by $w(x, t^0)$, where, on E_j,

$$w(x, t^0) = w_j^0(x(\xi)) = u_{j,0}^0 + u_{j,1}^0\,\xi. \tag{3.4}$$

Next, at time t^n, assume that the projection $w^n = w(x, t^n)$ is known, i.e., $u_{j,0}$ and $u_{j,1}$ are known for all j. We wish to calculate the cell average value $u_{j,0}^{n+1}$ and the scaled half slope $u_{j,1}^{n+1}$ at time t^{n+1}.

After advecting the piecewise linear data w a distance $a\Delta t$ to obtain v as in (2.10), the solution $u_{j,0}^{n+1}$ is given by (2.12). The scaled half slope update follows from (3.3) with t^n replaced by t^{n+1}, i.e.,

$$u_{j,1}^{n+1} = \frac{3}{2}\left(\int_{-1}^{-1+2\sigma} w_{j-1}(\xi - 2\sigma + 2)\,\xi\, d\xi + \int_{-1+2\sigma}^{1} w_j(\xi - 2\sigma)\,\xi\, d\xi \right). \tag{3.5}$$

A depiction of this process is shown in Fig. 3.1.

Carrying out the algebra, for scheme III, (2.12) implies

$$u_{j,0}^{n+1} = u_{j,0} + \sigma(-u_{j,0} - u_{j,1} + u_{j-1,0} + u_{j-1,1}) + \sigma^2(u_{j,1} - u_{j-1,1}), \tag{3.6}$$

and (3.5) results in

$$\begin{aligned} u_{j,1}^{n+1} = {} & u_{j,1} + 3\sigma\left(u_{j,0} - u_{j,1} - u_{j-1,0} - u_{j-1,1}\right) \\ & + 3\sigma^2\left(-u_{j,0} + u_{j-1,0} + 2u_{j-1,1}\right) + 2\sigma^3\left(u_{j,1} - u_{j-1,1}\right). \end{aligned} \tag{3.7}$$

Note that the term of highest degree for σ in (3.6) is σ^2 and that in (3.7) is σ^3.

The above can be written in matrix form for Fourier stability and accuracy analysis (later):

$$\begin{aligned} \begin{pmatrix} u_{j,0}^{n+1} \\ u_{j,1}^{n+1} \end{pmatrix} = {} & \begin{pmatrix} \sigma & \sigma(1-\sigma) \\ -3\sigma(1-\sigma) & -\sigma(3-6\sigma+2\sigma^2) \end{pmatrix} \begin{pmatrix} u_{j-1,0} \\ u_{j-1,1} \end{pmatrix} + \\ & \begin{pmatrix} 1-\sigma & -\sigma(1-\sigma) \\ 3\sigma(1-\sigma) & (1-\sigma)(1-2\sigma-2\sigma^2) \end{pmatrix} \begin{pmatrix} u_{j,0} \\ u_{j,1} \end{pmatrix} \end{aligned} \tag{3.8}$$

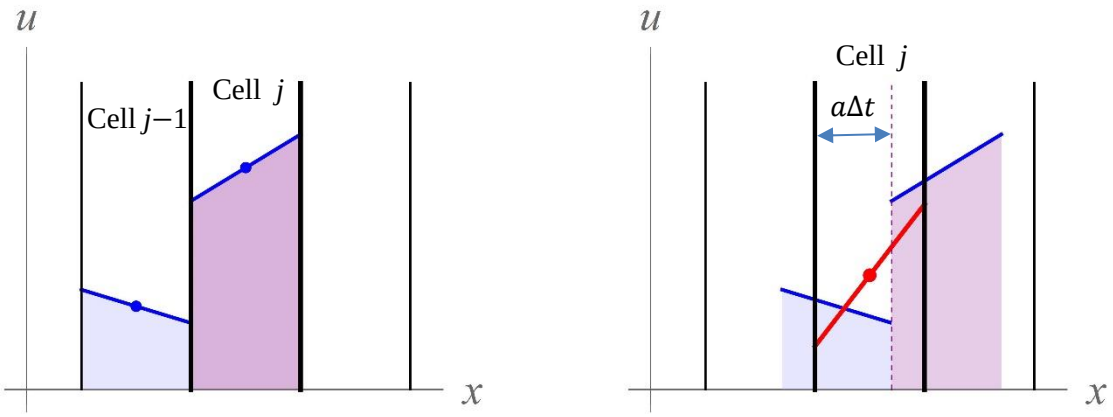

(a) Data (b) Solution

Figs. 3.1 Scheme III (a) Piecewise linear data defined by the cell average values (blue dots) and the (scaled half) slopes; (b) Solution obtained by shifting the data a distance corresponding to, in this case, $\sigma = 0.7$ and calculating the cell average value and the first moment of the discontinuous function (formed by the blue lines); the resulting linear solution is represented by the red dot and red line in cell j.

Whereas piecewise linear schemes are typically accurate to only second order, it will be shown by Von Neumann (Fourier) analysis that scheme III is third-order accurate and is stable for $0 \le \sigma \le 1$.

Scheme III can be considered as a piecewise linear DG scheme. In the case of one spatial dimension, its advantage is that for stability, the time step size limit corresponds to a CFL condition of 1. This condition, in fact, holds true to arbitrary degree of polynomial approximation. Such a CFL condition is a significant

gain compared to the standard DG method using explicit Runge-Kutta time stepping where, if p is the degree of the piecewise polynomial approximation, the time step size limit is proportional to $1/(1+p)^2$.

The final remark of this section concerns the extension to systems of equations. For the advection case, the discontinuity at an interface evolves via the exact shift operator. For the case of systems such as the Euler equations, in one spatial dimension, such a discontinuity gives rise to some combination of a shock, a contact, and a fan as time evolves. Tracking these waves accurately is extremely difficult. Resolving these waves for the multi-dimensional cases appears to be an impossible task. Extension of scheme III in a manner that avoids tracking these waves was carried out using a space-time Taylor series expansion by this author in (Huynh 2006, 2013) and Marcus Lo in his PhD dissertation under Van Leer (2011).

3.2 Van Leer's Scheme V

The key idea for this piecewise quadratic scheme is to define and update the quadratic solution in each cell using the interface and the cell average values. The method is described using the Legendre polynomials in (Van Leer 1977) and the Lagrange polynomials in (Eymann and Roe 2013). Here, for consistency with the high-order extension introduced later in Section 4, the Radau polynomials are employed.

At time t^n, assume that the cell average values $u_{j,0}^n = u_{j,0}$ and the interface values $u_{j+1/2}^n = u_{j+1/2}$ are known for all j. We wish to calculate $u_{j,0}^{n+1}$ and $u_{j+1/2}^{n+1}$ at time t^{n+1}. Note that the value $u_{j+1/2}$ is common for (or shared by) the two cells j and $j+1$.

On each cell E_j, let w_j be the parabola defined by the cell average value $u_{j,0}$ and the two interface values $u_{j-1/2}$ and $u_{j+1/2}$. It will be shown that w_j can be expressed as (3.13) below.

With ξ on $I = [-1, 1]$, let the left Radau polynomial of degree 2 denoted by $R_{L,2}$ be defined by:

$$R_{L,2}(-1) = 0, \quad R_{L,2}(1) = 1, \quad \text{and} \quad \int_{-1}^{1} R_{L,2}(\xi)\, d\xi = 0. \tag{3.9a,b,c}$$

A straightforward calculation yields

$$R_{L,2} = \frac{1}{4}(\xi + 1)(3\xi - 1). \tag{3.10}$$

Loosely put, the condition $R_{L,2}(1) = 1$ serves the purpose of taking on a certain value at the right interface, condition $R_{L,2}(-1) = 0$ leaves the value at the left interface unchanged, and condition $\int_{-1}^{1} R_{L,2}(\xi)\, d\xi = 0$ leaves the cell average quantity unchanged. In a similar manner, let the right Radau polynomial of degree 2 denoted by $R_{R,2}$ be defined by applying a reflection to $R_{L,2}$,

$$R_{R,2}(-1) = 1, \quad R_{R,2}(1) = 0, \quad \text{and} \quad \int_{-1}^{1} R_{R,2}(\xi)\, d\xi = 0. \tag{3.11a,b,c}$$

Replacing ξ by $-\xi$ in (3.10), we obtain

$$R_{R,2} = \frac{1}{4}(\xi - 1)(3\xi + 1). \tag{3.12}$$

The parabola w_j determined by $u_{j,0}$, $u_{j-1/2}$, and $u_{j+1/2}$ can be written as

$$w_j(\xi) = u_{j,0} + (u_{j+1/2} - u_{j,0})R_{L,2}(\xi) + (u_{j-1/2} - u_{j,0})R_{R,2}(\xi). \tag{3.13}$$

Indeed, both $R_{L,2}$ and $R_{R,2}$ have zero average value on I; as a result, the cell average value of the right hand side above is $u_{j,0}$. In addition, by (3.9a,b) and (3.11a,b),

$$w_j(-1) = u_{j-1/2} \quad \text{and} \quad w_j(1) = u_{j+1/2}.$$

With w_j defined by (3.13), the piecewise parabolic data $w(x) = \{w_j(x)\}$ at time level t^n is continuous across cell interfaces. The solution at time t^{n+1} is obtained by shifting the data curve to the right a distance $a\Delta t$,

$$w(x - a\Delta t) = w(x - \sigma\Delta x).$$

The cell average update is given by (2.11). The interface value is updated by

$$u_{j+1/2}^{n+1} = w_j(1 - 2\sigma). \tag{3.14}$$

A depiction of this process is shown in Fig. 3.2.

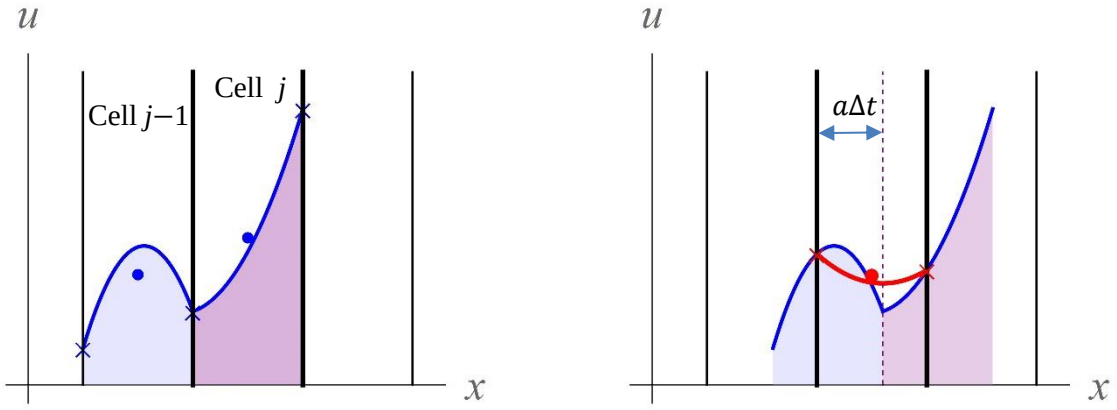

(a) Data (b) Solution

Fig. 3.2 Scheme V. (a) Piecewise quadratic data determined by, in each cell, the two interface values (blue crosses) and the cell average value (blue dots); (b) Solution in cell j obtained by (1) shifting the data a distance corresponding to, in this case, $\sigma = 0.6$ and (2) calculating the cell average value of the piecewise polynomial function in cell j (red dot), and obtaining the interface value updates (two red crosses).

After some algebra, for scheme V, the cell average update is

$$\begin{aligned} u_{j,0}^{n+1} = \; & u_{j,0} + \sigma(-u_{j+1/2} + u_{j-1/2}) \\ & + \sigma^2(-3u_{j,0} + 3u_{j-1,0} + 2u_{j+1/2} - u_{j-1/2} - u_{j-3/2}) \\ & + \sigma^3(2u_{j,0} - 2u_{j-1,0} - u_{j+1/2} + u_{j-3/2}), \end{aligned} \tag{3.15}$$

and the interface value update is

$$u_{j+1/2}^{n+1} = 6\sigma(1-\sigma)u_{j,0} + (1-\sigma)(1-3\sigma)u_{j+1/2} + \sigma(-2+3\sigma)u_{j-1/2}\,. \tag{3.16}$$

For Von Neumann (Fourier) stability and accuracy analysis, the solution is written in matrix form. In the cell j, the cell average $u_{j,0}$ and the right interface value $u_{j+1/2}$ are grouped together. The update for scheme V involves the data in three cells, from $j-2$ to j,

$$\begin{aligned}\begin{pmatrix} u_{j,0}^{n+1} \\ u_{j+1/2}^{n+1} \end{pmatrix} = & \begin{pmatrix} 0 & -\sigma^2(1-\sigma) \\ 0 & 0 \end{pmatrix}\begin{pmatrix} u_{j-2,0} \\ u_{j-3/2} \end{pmatrix} + \\ & \begin{pmatrix} \sigma^2(3-2\sigma) & \sigma(1-\sigma) \\ 0 & \sigma(-2+3\sigma) \end{pmatrix}\begin{pmatrix} u_{j-1,0} \\ u_{j-1/2} \end{pmatrix} + \\ & \begin{pmatrix} (1-\sigma)^2(1+2\sigma) & -\sigma(1-\sigma)^2 \\ 6\sigma(1-\sigma) & (1-\sigma)(1-3\sigma) \end{pmatrix}\begin{pmatrix} u_{j,0} \\ u_{j+1/2} \end{pmatrix}. \end{aligned} \tag{3.17}$$

3.3 Equivalence of Van Leer's Schemes III and V

The equivalence of the above two schemes, a key result of this paper, can now be stated and proved.

At time t^n, assume that the data for scheme V are known, i.e., $u_{j,0}$ and $u_{j+1/2}$ are known for all j; in addition, the CFL number σ is fixed. For scheme III, set

$$u_{j,1} = (1-\sigma)\big(u_{j+1/2} - u_{j,0}\big) + \sigma\big(u_{j,0} - u_{j-1/2}\big). \tag{3.18}$$

Then at time t^{n+1}, the cell average solution by schemes III is identical to that by scheme V:

$$u_{j,0}^{n+1,\,\mathrm{III}} = u_{j,0}^{n+1,\,\mathrm{V}}. \tag{3.19}$$

Abbreviate the above to $u_{j,0}^{n+1}$, $u_{j,1}^{n+1,\,\mathrm{III}}$ to $u_{j,1}^{n+1}$, and $u_{j+1/2}^{n+1,\,\mathrm{V}}$ to $u_{j+1/2}^{n+1}$. In addition to the identical solution averages, the scaled half slope update by scheme III and interface value update by scheme V satisfy an expression similar to (3.18):

$$u_{j,1}^{n+1} = (1-\sigma)\big(u_{j+1/2}^{n+1} - u_{j,0}^{n+1}\big) + \sigma\big(u_{j,0}^{n+1} - u_{j-1/2}^{n+1}\big). \tag{3.20}$$

Proof. To prove (3.19), consider the cell average update by scheme III given by (3.6). Substitute $u_{j,1}$ by the right hand side of (3.18) and $u_{j-1,1}$ by the same quantity with j replaced by $j-1$ into (3.6) (these quantities appear in the square brackets below), we obtain

$$\begin{aligned} u_{j,0}^{n+1,\,\mathrm{III}} = \; & u_{j,0} \\ & + \sigma\Big\{ u_{j-1,0} + \big[(1-\sigma)\big(u_{j-1/2} - u_{j-1,0}\big) + \sigma\big(u_{j-1,0} - u_{j-3/2}\big)\big] \\ & \quad - u_{j,0} - \big[(1-\sigma)\big(u_{j+1/2} - u_{j,0}\big) + \sigma\big(u_{j,0} - u_{j-1/2}\big)\big]\Big\} \\ & + \sigma^2\Big\{\big[(1-\sigma)\big(u_{j+1/2} - u_{j,0}\big) + \sigma\big(u_{j,0} - u_{j-1/2}\big)\big] \; - \\ & \quad \big[(1-\sigma)\big(u_{j-1/2} - u_{j-1,0}\big) + \sigma\big(u_{j-1,0} - u_{j-3/2}\big)\big]\Big\}. \end{aligned} \tag{3.21}$$

After simplification, the above yields a result identical to (3.15), the cell average solution of scheme V. Thus, (3.19) holds.

To prove (3.20), consider the scaled half slope update (3.7). Again, substitute $u_{j,1}$ by the right hand side of (3.18) and $u_{j-1,1}$ by the same quantity with j replaced by $j-1$ into (3.7), we obtain

$$\begin{aligned} u_{j,1}^{n+1,\mathrm{III}} = {} & \left[(1-\sigma)\left(u_{j+1/2}-u_{j,0}\right)+\sigma\left(u_{j,0}-u_{j-1/2}\right)\right] + \\ & 3\sigma\left\{u_{j,0}-\left[(1-\sigma)\left(u_{j+1/2}-u_{j,0}\right)+\sigma\left(u_{j,0}-u_{j-1/2}\right)\right]-u_{j-1,0}\right. \\ & \left.-\left[(1-\sigma)\left(u_{j-1/2}-u_{j-1,0}\right)+\sigma\left(u_{j-1,0}-u_{j-3/2}\right)\right]\right\} + \\ & 3\sigma^2\left\{-u_{j,0}+u_{j-1,0}+2\left[(1-\sigma)\left(u_{j-1/2}-u_{j-1,0}\right)+\sigma\left(u_{j-1,0}-u_{j-3/2}\right)\right]\right\} \\ & +2\sigma^3\left\{\left[(1-\sigma)\left(u_{j+1/2}-u_{j,0}\right)+\sigma\left(u_{j,0}-u_{j-1/2}\right)\right]\right. \\ & \left.-\left[(1-\sigma)\left(u_{j-1/2}-u_{j-1,0}\right)+\sigma\left(u_{j-1,0}-u_{j-3/2}\right)\right]\right\} \end{aligned} \tag{3.22}$$

where the quantities in the square brackets are either $u_{j,1}$ or $u_{j-1,1}$. After simplification,

$$\begin{aligned} u_{j,1}^{n+1,\mathrm{III}} = {} & u_{j+1/2}-u_{j,0}+\ 4\sigma\left(2u_{j,0}-u_{j+1/2}-u_{j-1/2}\right) \\ & +3\sigma^2\left(-3u_{j,0}-3u_{j-1,0}+u_{j+1/2}+4u_{j-1/2}+u_{j-3/2}\right) \\ & +2\sigma^3\left(-u_{j,0}+7u_{j-1,0}+u_{j+1/2}-4u_{j-1/2}-3u_{j-3/2}\right) \\ & +2\sigma^4\left(2u_{j,0}-2u_{j-1,0}-u_{j+1/2}+u_{j-3/2}\right). \end{aligned} \tag{3.23}$$

Denote the right hand side of (3.20) by $\mathrm{RHS}_{(3.20)}$. With the interface value update $u_{j+1/2}^{n+1}$ for scheme V given by (3.16) and cell average update $u_{j,0}^{n+1}$ for both schemes by (3.15),

$$\begin{aligned} \mathrm{RHS}_{(3.20)} = {} & (1-\sigma)\left\{\left[6\sigma(1-\sigma)u_{j,0}+(1-\sigma)(1-3\sigma)u_{j+1/2}+\ \sigma(-2+3\sigma)u_{j-1/2}\right]\right. \\ & -\ \left[u_{j,0}-\sigma\left(u_{j+1/2}-u_{j-1/2}\right)\right. \\ & +\sigma^2\left(-3u_{j,0}+\ 3u_{j-1,0}+2u_{j+1/2}-u_{j-1/2}-u_{j-3/2}\right) \\ & \left.\left.+\ \sigma^3\left(2u_{j,0}-2u_{j-1,0}-u_{j+1/2}+u_{j-3/2}\right)\right]\right\} \\ & +\ \sigma\left\{\left[u_{j,0}-\sigma\left(u_{j+1/2}-u_{j-1/2}\right)\right.\right. \\ & +\sigma^2\left(-3u_{j,0}+\ 3u_{j-1,0}+2u_{j+1/2}-u_{j-1/2}-u_{j-3/2}\right) \\ & \left.+\ \sigma^3\left(2u_{j,0}-2u_{j-1,0}-u_{j+1/2}+u_{j-3/2}\right)\right] \\ & \left.-\left[6\sigma(1-\sigma)u_{j-1,0}+(1-\sigma)(1-3\sigma)u_{j-1/2}+\ \sigma(-2+3\sigma)u_{j-3/2}\right]\right\}. \end{aligned}$$

After simplification, the above is identical to (3.23). This completes the equivalence proof.

3.4 Examples

Two examples concerning the above equivalence are in order, the first for σ near 0, and the second, σ near 1. Note that if σ approaches 0, then $u_{j,1}$ defined by (3.18) approaches $u_{j+1/2}-u_{j,0}$, and the corresponding linear approximation is downwind biased in the j-th cell (Fig. 3.3(c) below). On the other hand, if σ approaches 1, then $u_{j,1}$ approaches $u_{j,0}-u_{j-1/2}$, and the corresponding linear approximation is upwind biased (Fig. 3.4(a)).

Suppose the continuous piecewise quadratic data for the cells $j-1$ and j are given as in Fig. 3.3(a).

First, set $\sigma = 0.2$ (close to 0). After one time step, the solution by scheme V for the cell j is shown in Fig. 3.3(b). From the parabolic data in Fig. 3.3(a), let the scaled half slope $u_{j,1}$ be defined by the weighted

average (3.18). The resulting piecewise linear data is shown in Fig. 3.3(c). Note its downwind bias (due to the fact that σ is close to 0). After one time step corresponding to $\sigma = 0.2$, the linear solution by scheme III as well as the parabolic solution by scheme V are shown in Fig. 3.3(d). Here, the cell average solutions by the two schemes are identical. In addition, in a manner similar to the relation (3.18) between the linear and parabolic data, for the solution, the scaled half slope update $u_{j,1}^{n+1,\mathrm{III}}$ and the interface value update $u_{j+1/2}^{n+1,\mathrm{V}}$ satisfy the weighted average relation (3.20) with $\sigma = 0.2$.

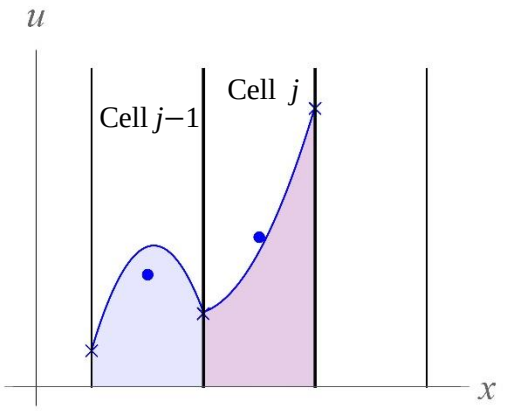

(a) Piecewise parabolic data for scheme V

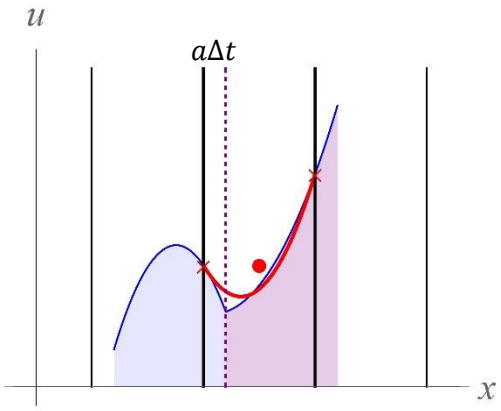

(b) Solution by scheme V with $\sigma = 0.2$

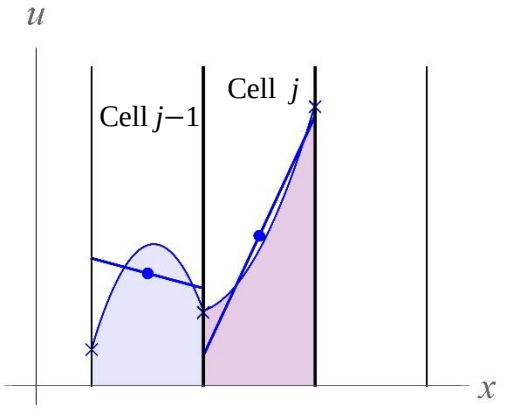

(c) Piecewise Linear Data with $u_{j,1}$ via (3.18)

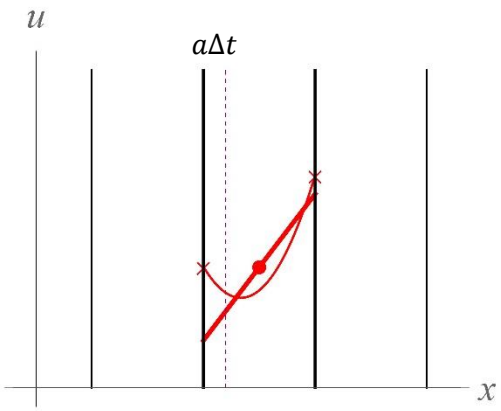

(d) Solutions by schemes III and V

Figs. 3.3 Equivalence of schemes III and V for $\sigma = 0.2$. (a) Piecewise parabolic data. (b) Solution in cell j by scheme V for $\sigma = 0.2$. (c) Piecewise linear data with $u_{j,1}$ given by the weighted average (3.18); note the downwind bias of the linear functions relative to the parabolic data since σ is close to 0. (d) Solutions in cell j by schemes III and V; here, the two cell average solutions are identical; in addition, $u_{j,1}^{n+1,\mathrm{III}}$, $u_{j,0}^{n+1}$, and $u_{j+1/2}^{n+1,\mathrm{V}}$ satisfy relation (3.20) with $\sigma = 0.2$.

Next, set $\sigma = 0.8$ (close to 1). With $u_{j,1}$ defined by (3.18), the resulting piecewise linear data and the original piecewise parabolic data are shown in Fig. 3.4(a). Note the upwind bias of the linear data since σ

is close to 1. After one time step with $\sigma = 0.8$, the solutions by schemes III and V for the cell j are shown in Fig. 3.4(b). The two cell average solutions are identical; in addition, $u_{j,1}^{n+1,\mathrm{III}}$ and $u_{j+1/2}^{n+1,\mathrm{V}}$ satisfy (3.20) with $\sigma = 0.8$.

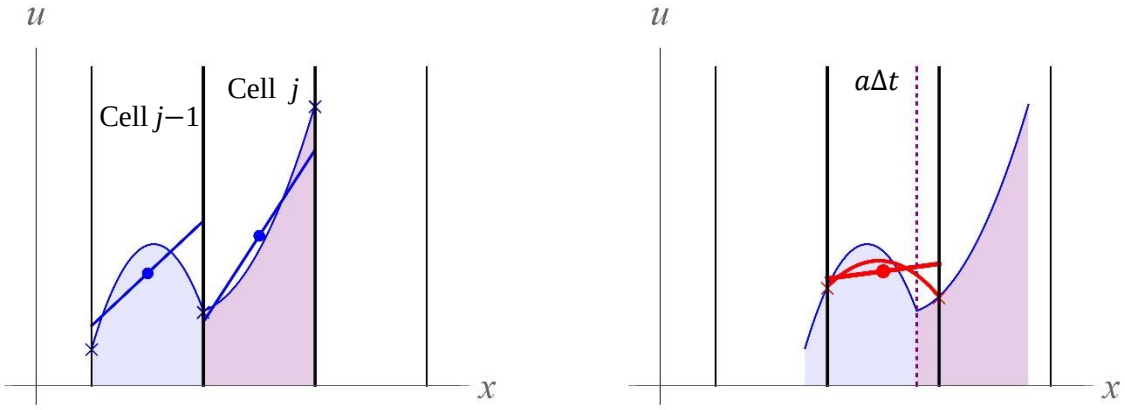

(a) Parabolic and linear data with $\sigma = 0.8$ (b) Solution by schemes III and V for $\sigma = 0.8$

Figs. 3.4 Equivalence of schemes III and V for $\sigma = 0.8$. (a) Piecewise quadratic and piecewise linear data with $u_{j,1}$ given by the weighted average (3.18); note the upwind bias of the linear functions due to the fact that σ is close to 1. (b) Solutions in cell j by schemes III and V. Here, the two cell average solutions are identical; in addition, $u_{j,1}^{n+1,\mathrm{III}}$, $u_{j,0}^{n+1}$, and $u_{j+1/2}^{n+1,\mathrm{V}}$ satisfy (3.20) with $\sigma = 0.8$.

The final observation for this section concerns the initial data. For scheme III, based on the idea of obtaining the solution by projecting onto the space of piecewise linear functions, it is sensible to define the initial piecewise linear data by projecting the initial condition as discussed in (3.4). However, due to the above equivalence between schemes III and V, if the CFL number σ is fixed, a better choice for the initial data for scheme III that assures third-order accuracy of the (cell average) solution is the following. At time t^0, assume that the cell average values $u_{j,0}^0$ and the cell interface values $u_{j+1/2}^0$ for scheme V are given for all j, and they are highly accurate (third or higher order). Then the solution by scheme V after N time steps is third-order accurate. Using (3.8), we can define the initial scaled half slope $u_{j,1}^0$ for scheme III by

$$u_{j,1}^0 = \sigma\left(u_{j+1/2}^0 - u_{j,0}^0\right) + (1-\sigma)\left(u_{j,0}^0 - u_{j-1/2}^0\right). \tag{3.24}$$

With such initial data, the solutions by schemes III and V at the final time t^N are identical in the sense that (a) the cell average solutions for both schemes are the same and (b) the final scaled half slopes of scheme III relate to the final interface values of scheme V via an expression similar to (3.20) for the final time t^N.

4 High-Order Extensions of Schemes for Advection

A framework using both projection and interpolation that extends schemes III and V into a family of arbitrary order schemes is introduced below.

4.1 Notations and Review

We need some notations as well as the definition and a few key properties of the Legendre polynomials.

On the reference interval $I = [-1, 1]$, let the inner product of two functions v_1 and v_2 be defined by

$$(v_1, v_2) = \int_{-1}^{1} v_1(\xi)\, v_2(\xi)\, d\xi, \tag{4.1}$$

and the L_2 norm of a function v by

$$\|v\| = \left(\int_{-1}^{1} \big(v(\xi)\big)^2\, d\xi \right)^{1/2}. \tag{4.2}$$

For any nonnegative integer k, denote by $\boldsymbol{P}_k$ the space of polynomials of degree $\leq k$. Let the Legendre polynomial L_k be defined as the unique polynomial of degree k that is orthogonal to $\boldsymbol{P}_{k-1}$ and $L_k(1) = 1$. The Legendre polynomials are given by a recurrence formula (e.g., Hildebrand 1987):

$$L_0(\xi) = 1, \quad L_1(\xi) = \xi, \tag{4.3}$$

and, for $k \geq 2$,

$$L_k(\xi) = \frac{2k-1}{k} \xi\, L_{k-1}(\xi) - \frac{k-1}{k} L_{k-2}(\xi). \tag{4.4}$$

It is well known that,

$$\|L_k\|^2 = (L_k, L_k) = \frac{2}{2k+1}. \tag{4.5}$$

The first few Legendre polynomials are: L_0, L_1 in (4.3),

$$L_2(\xi) = \frac{1}{2}(3\xi^2 - 1), \quad L_3(\xi) = \frac{1}{2}(5\xi^3 - 3\xi), \quad \text{and} \quad L_4(\xi) = \frac{1}{8}(35\xi^4 - 30\xi^2 + 3).$$

Their plots are shown in Fig. 4.1.

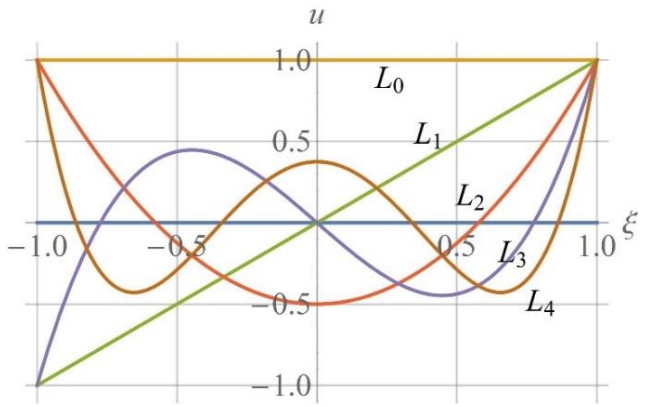

Fig. 4.1 Legendre polynomials

For any integer $m \geq 0$, let $\mathcal{P}_m$ be the projection onto $\boldsymbol{P}_m$, i.e., for any integrable function v,

$$\mathcal{P}_m(v) = \sum_{k=0}^{m} \frac{(v, L_k)}{\|L_k\|^2} L_k = \sum_{k=0}^{m} \frac{2k+1}{2} (v, L_k) L_k. \tag{4.6}$$

4.2 PμIν Scheme

The following approach extends both schemes III and V into a PμIν family where 'P' stands for projection, 'I' for interpolation (Hermite type), and μ and ν are integers with $\mu \geq -1$ and $\nu \geq -1$.

At time t^n, in each cell E_j, the projection of the data onto $\boldsymbol{P}_\mu$ results in the $\mu + 1$ quantities

$$u_{j,k}^n = u_{j,k}, \ 0 \leq k \leq \mu \tag{4.7}$$

where, by (4.6),

$$u_{j,k} \approx \frac{2k+1}{2} (u, L_k). \tag{4.8}$$

If $\mu = -1$, then $\boldsymbol{P}_{-1} = \{0\}$, and the projection part vanishes.

For the interpolation part, if $\nu = -1$, it is nonexistent. If $\nu \geq 0$, at each interface $x_{j+1/2}$, the interpolation part consists of approximations to $\frac{d^l u}{d\xi^l}$ up to degree ν, namely, the $\nu + 1$ quantities

$$u_{j+1/2,l}^n = u_{j+1/2,l}, \ 0 \leq l \leq \nu. \tag{4.9}$$

The interface values are $u_{j+1/2,0}^n = u_{j+1/2}$. Note that the time level is fixed, so we use the notation d instead of ∂. In practice, typically, $u_{j+1/2,l}$ approximates $\frac{d^l u}{dx^l}$, but since $\frac{d^l u}{d\xi^l}$ relates to $\frac{d^l u}{dx^l}$ by the chain rule in a straightforward manner, for convenience, $u_{j+1/2,l}$ approximates $\frac{d^l u}{d\xi^l}$ here.

Again at time t^n, assume that the data $u_{j,k}$ and $u_{j+1/2,l}$ are known for all j, k, and l. We wish to calculate $u_{j,k}^{n+1}$ and $u_{j+1/2,l}^{n+1}$ at time t^{n+1}.

In each cell, the interface quantities at the two boundaries provide $2(\nu + 1)$ conditions and the projection part provides $\mu + 1$ conditions. Thus, the total number of conditions for each cell is $\mu + 1 + 2(\nu + 1)$ resulting in a polynomial of degree $\mu + 2(\nu + 1)$.

On E_j, let w_j be the polynomial of degree $\mu + 2(\nu + 1)$ defined by the $\mu + 1$ Legendre coefficients $u_{j,k}$ and the $2(\nu + 1)$ interface quantities $u_{j-1/2,l}$ and $u_{j+1/2,l}$. The polynomial w_j is expressed using the Legendre polynomials for the projection part and the basis functions $\phi_{L,l}$ and $\phi_{R,l}$ below for the interpolation part.

Let $\phi_{L,l}$ be the polynomial of degree $\mu + 2(\nu + 1)$ defined on $I = [-1, 1]$ so that it is orthogonal to $\boldsymbol{P}_\mu$, and all derivatives of degree $\leq \nu$ at the two boundaries vanish except

$$\frac{d^l \phi_{L,l}}{d\xi^l}(-1) = 1. \tag{4.10}$$

Let $\phi_{R,l}$ be defined in the same manner except, at the right boundary,

$$\frac{d^l \phi_{R,l}}{d\xi^l}(1) = 1. \tag{4.11}$$

An example for $\phi_{L,l}$ and $\phi_{R,l}$ for the case $\mu = 0$ and $\nu = 2$ is shown in Fig. 4.2. Note that on I, the maximum value of $|\phi_{L,l}|$ and $|\phi_{R,l}|$ gets smaller fast as l increases; here, again on I, $\max|\phi_{L,1}| = \max|\phi_{R,1}| \approx 0.22$ and $\max|\phi_{L,2}| = \max|\phi_{R,2}| \approx 0.02$.

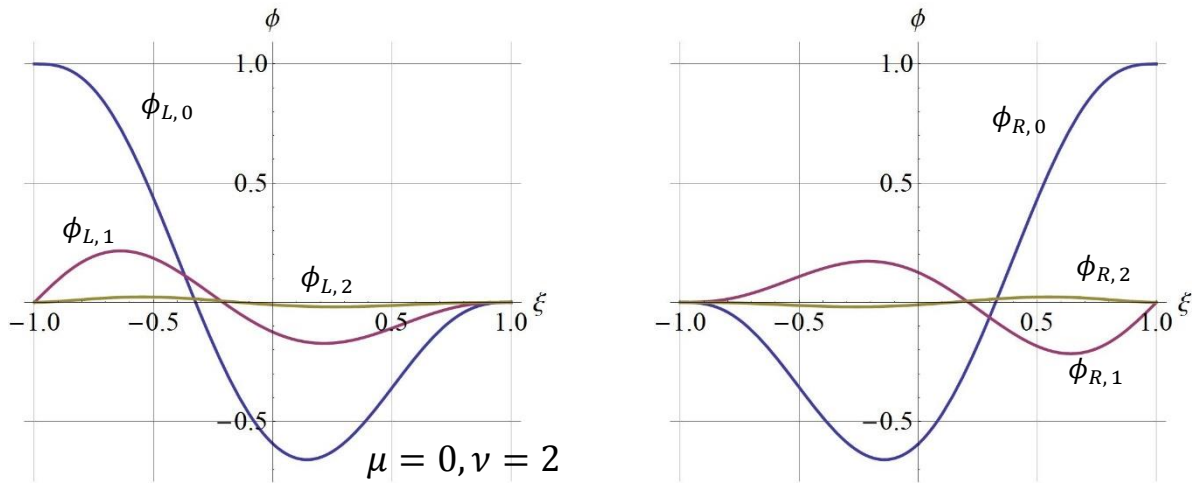

(a) Basis functions $\phi_{L,l}$, $0 \le l \le 2$ (b) Basis functions $\phi_{R,l}$, $0 \le l \le 2$

Fig. 4.2 Basis functions $\phi_{L,l}$ and $\phi_{R,l}$ for the case $\mu = 0$, $\nu = 2$.

For $\phi_{L,l}$, since all derivatives of degree $\le \nu$ at the right boundary vanish,

$$\phi_{L,l}(\xi) = (\xi - 1)^{\nu+1} p(\xi)$$

where p is of degree $\mu + \nu + 1$. Similarly,

$$\phi_{R,l} = (\xi + 1)^{\nu+1} r(\xi)$$

where r is of degree $\mu + \nu + 1$.

Also note that the function $\phi_{R,l}(\xi) - (-1)^l \phi_{L,l}(-\xi)$ is orthogonal to $\boldsymbol{P}_\mu$, and all derivatives of degree $\le \nu$ at the two boundaries vanish. Therefore, it is identically zero, i.e.,

$$\phi_{R,l}(\xi) = (-1)^l \phi_{L,l}(-\xi). \tag{4.12}$$

The polynomial w_j can now be expressed using the above basis functions: with

$$p_j(\xi) = \sum_{k=0}^{\mu} u_{j,k} L_k(\xi), \tag{4.13}$$

and with $p_j^{(m)} = \frac{d^m}{d\xi^m} p_j$, set

$$\begin{aligned} w_j(\xi) = p_j(\xi) &+ \sum_{l=0}^{\nu} \left(u_{j-1/2,\,l} - p_j^{(l)}(-1) \right) \phi_{L,\,l}(\xi) \\ &+ \sum_{l=0}^{\nu} \left(u_{j+1/2,\,l} - p_j^{(l)}(1) \right) \phi_{R,\,l}(\xi). \end{aligned} \tag{4.14}$$

The above w_j has the desired projection and interpolation properties. Indeed, for the projection part, since $\phi_{L,\,l}$ and $\phi_{R,\,l}$ are orthogonal to $\boldsymbol{P}_\mu$,

$$\mathcal{P}_\mu(w_j) = \mathcal{P}_\mu(p_j) = p_j. \tag{4.15}$$

For the interpolation part, by (4.10) and (4.11) respectively,

$$\frac{d^l w_j}{d\xi^l}(-1) = u_{j-1/2,\,l} \quad \text{and} \quad \frac{d^l w_j}{d\xi^l}(1) = u_{j+1/2,\,l}. \tag{4.16}$$

At time t^{n+1}, the shifted solution is $w(x - a\Delta t) = w(x - \sigma\Delta x)$. The solutions of the projection part are given by, for $0 \le k \le \mu$,

$$u_{j,k}^{n+1} = \frac{2k+1}{2} \left(\int_{-1}^{-1+2\sigma} w_{j-1}(\xi - 2\sigma + 2)\, L_k(\xi)\, d\xi + \int_{-1+2\sigma}^{1} w_j(\xi - 2\sigma)\, L_k(\xi)\, d\xi \right). \tag{4.17}$$

Concerning the interpolation part, for $0 \le l \le \nu$, the interface quantities are updated by

$$u_{j+1/2,\,l}^{n+1} = \frac{d^l w_j}{d\xi^l}(1 - 2\sigma) = w_j^{(l)}(1 - 2\sigma). \tag{4.18}$$

This completes the description of the PμIν method.

The solutions (4.17) and (4.18) for the PμIν method as functions of $u_{j-3/2,\,l}$, $u_{j-1,\,k}$, $u_{j-1/2,\,l}$, $u_{j,\,k}$, $u_{j+1/2,\,l}$, and the CFL number σ can be obtained using a software package such as Mathematica or Matlab.

For these schemes, if $\nu = -1$, the interpolation part becomes nonexistent, and the resulting method involves only projection and is called the Pμ scheme (instead of PμI(-1)). On the other hand, if $\mu = -1$, the projection part becomes nonexistent, and the resulting method is an interpolation scheme denoted by Iν; since an interpolation scheme involves no projection, it has the drawback of being non-conservative and therefore cannot capture shocks.

Also note that at each interface, the derivatives up to degree ν are shared by the two adjacent cells, consequently, the piecewise polynomial function in the PμIν method is C^ν continuous, i.e., derivatives of degree up to ν are continuous.

4.3 PμIν Schemes with a Fixed Number of Degrees of Freedom

Let K be the number of degrees of freedom in each cell that includes the $(\mu + 1)$ pieces of data for the projection part and the $(\nu + 1)$ pieces for the interpolation part at the right boundary (but not left). That is,

$$K = \mu + \nu + 2.$$

With $K \geq 1$ fixed, consider all $\mu \geq -1$ and $\nu \geq -1$ that satisfy

$$\mu + \nu = K - 2. \tag{4.19}$$

Such PμIν schemes, which are piecewise polynomial of degree $\mu + 2(\nu + 1)$, include:

$$\text{P}(K-1), \text{P}(K-2)\text{I0}, \text{P}(K-3)\text{I1}, \ldots, \text{P1I}(K-3), \text{P0I}(K-2), \text{and I}(K-1). \tag{4.20}$$

These schemes have the following remarkable property. They all share the same sets of eigenvalues and thus, have the same stability and accuracy as will be discussed in the next section.

Note that there are a total of $K + 1$ schemes in the family. Loosely put, each scheme in (4.20) is obtained from the previous member in the list by moving one degree of freedom from the projection part to the interpolation part.

The following cases for (4.20) are in order.

(1) $K = 1$, then P0 is the first-order upwind scheme, and I0 the first-order (linear) interpolation scheme.

(2) $K = 2$, then P1 is scheme III (linear), P0I0 is scheme V (parabolic), and I1 is a C^1 piecewise cubic method.

(3) $K = 3$, then P2 is Van Leer's scheme VI (parabolic), P1I0 a C^0 piecewise cubic method, P0I1 a C^1 piecewise polynomial of degree 4, and I2 a C^2 piecewise polynomial of degree 5.

5 Von Neumann (or Fourier) Stability and Accuracy Analysis

Consider the advection equation (2.1) with $a \geq 0$. Let the cells be $E_j = [j - 1/2, j + 1/2]$. For the PμIν schemes, denote by $\boldsymbol{U}_j$ the column vector of $K = \mu + \nu + 2$ components obtained by joining the projection data $u_{j,k},\ 0 \leq k \leq \mu$ and the interpolation data at the right interface $u_{j+1/2,l},\ 0 \leq l \leq \nu$:

$$\boldsymbol{U}_j = \left(u_{j,0}, u_{j,1}, \ldots, u_{j,\,\mu+\nu+1}\right)^T \tag{5.1}$$

where $u_{j,\,\mu+1} = u_{j+1/2,\,0}$, …, and T represents the transpose.

Next, let Δt be the time step; since $\Delta x = 1$, $\sigma = a\Delta t$. Assume that the data $\boldsymbol{U}_j^n = \boldsymbol{U}_j$ are known. For the PμIν schemes, the solution $\boldsymbol{U}_j^{n+1}$ via (4.17) and (4.18) can be expressed as

$$\boldsymbol{U}_j^{n+1} = \boldsymbol{C}_{-2}\boldsymbol{U}_{j-2} + \boldsymbol{C}_{-1}\boldsymbol{U}_{j-1} + \boldsymbol{C}_0\boldsymbol{U}_j \tag{5.2}$$

where $\boldsymbol{C}_{-2}$, $\boldsymbol{C}_{-1}$, and $\boldsymbol{C}_0$ are $K \times K$ matrices depending on σ. Note that $\boldsymbol{C}_{-2} = 0$ for the P and the I schemes.

As examples, for P1, by (3.8),

$$\boldsymbol{C}_{-1} = \begin{pmatrix} \sigma & \sigma(1-\sigma) \\ -3\sigma(1-\sigma) & -\sigma(3-6\sigma+2\sigma^2) \end{pmatrix} \text{ and } \boldsymbol{C}_0 = \begin{pmatrix} 1-\sigma & \sigma(1-\sigma) \\ -3\sigma(1-\sigma) & (1-\sigma)(-1+2\sigma+2\sigma^2) \end{pmatrix}.$$

For scheme V or P0I0, by (3.17),

$$\boldsymbol{C}_{-2} = \begin{pmatrix} 0 & -\sigma^2(1-\sigma) \\ 0 & 0 \end{pmatrix}, \qquad \boldsymbol{C}_{-1} = \begin{pmatrix} \sigma^2(3-2\sigma) & \sigma(1-\sigma) \\ 0 & \sigma(-2+3\sigma) \end{pmatrix},$$

and

$$\boldsymbol{C}_0 = \begin{pmatrix} (1-\sigma)^2(1+2\sigma) & -\sigma(1-\sigma)^2 \\ 6\sigma(1-\sigma) & (1-\sigma)(1-3\sigma) \end{pmatrix}.$$

For P2 or the parabolic projection scheme,

$$\boldsymbol{C}_{-1} = \begin{pmatrix} \sigma & \sigma(1-\sigma) & \sigma(1-\sigma)(1-2\sigma) \\ -3\sigma(1-\sigma) & -\sigma(3-6\sigma+2\sigma^2) & -3\sigma(1-\sigma)(1-3\sigma+\sigma^2) \\ 5\sigma(1-\sigma)(1-2\sigma) & 5\sigma(1-\sigma)(1-3\sigma+\sigma^2) & \sigma(5-30\sigma+50\sigma^2-30\sigma^3+6\sigma^4) \end{pmatrix},$$

and

$$\boldsymbol{C}_0 = \begin{pmatrix} 1-\sigma & -\sigma(1-\sigma) & -\sigma(1-\sigma)(1-2\sigma) \\ 3\sigma(1-\sigma) & (1-\sigma)(1-2\sigma-2\sigma^2) & -3\sigma(1-\sigma)(1-\sigma-\sigma^2) \\ -5\sigma(1-\sigma)(1-2\sigma) & 5\sigma(1-\sigma)(1-\sigma-\sigma^2) & (1-\sigma)(1-4\sigma-4\sigma^2+6\sigma^3+6\sigma^4) \end{pmatrix}.$$

Note the term of highest degree for σ is σ^5, consistent with the fifth-order accuracy of this scheme discussed later.

Stability.

Let w be the wave number such that $-\pi < w \leq \pi$, and the imaginary unit be i. For Fourier stability analysis, assume that the solution satisfies, for all j,

$$\boldsymbol{U}_j = e^{ijw}\boldsymbol{U}_0.$$

This assumption replaces that of $u_j = e^{ijw}u_0$ in the finite-volume and finite-difference methods. Equivalently,

$$\boldsymbol{U}_{j-1} = e^{-iw}\boldsymbol{U}_j. \tag{5.3}$$

By (5.2), set

$$\boldsymbol{A} = e^{-2iw}\boldsymbol{C}_{-2} + e^{-iw}\boldsymbol{C}_{-1} + \boldsymbol{C}_0. \tag{5.4}$$

Recall that $\boldsymbol{U}_j = \boldsymbol{U}_j^n$. By (5.2) and (5.3),

$$\boldsymbol{U}_j^{n+1} = \boldsymbol{A}\boldsymbol{U}_j = \boldsymbol{A}\boldsymbol{U}_j^n. \tag{5.5}$$

That is, $\boldsymbol{A}$ is the amplification matrix. As a result of the above, if $\boldsymbol{U}_j^0$ is the initial data, then $\boldsymbol{U}_j^{n+1} = \boldsymbol{A}^{n+1}\boldsymbol{U}_j^0$.

For each value of σ and w where $0 \le \sigma \le 1$ and $-\pi < w \le \pi$, $\boldsymbol{A}$ is a $K \times K$ matrix with K complex eigenvalues. For stability, all of these K values must have magnitude ≤ 1 as σ and w vary.

Based on numerical calculations of these eigenvalues tested by this author, all PμIν schemes are stable. The following plots show the magnitude of the K eigenvalues (or amplification factors) for $0 \le \sigma \le 1$ and, due to symmetry, $-\pi < w \le 0$.

For $K = 1$, the P0 (first-order upwind) and, using convention (5.1), the I0 (first-order interpolation) schemes both result in

$$u_j^{n+1} = \sigma u_{j-1} + (1-\sigma)u_j.$$

Thus, $\boldsymbol{C}_{-1} = \sigma$ and $\boldsymbol{C}_0 = 1 - \sigma$; consequently,

$$\boldsymbol{A} = \sigma e^{-iw} + 1 - \sigma = 1 + \sigma(e^{-iw} - 1).$$

The amplification factor $\boldsymbol{A}$ is shown in Fig. 5.1(a). Its magnitude |Amp| as function of σ and w is plotted in Fig. 5.1(b).

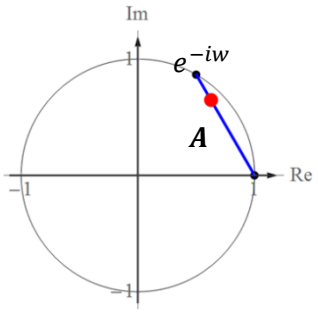

(a) Amplification factor $\boldsymbol{A}$

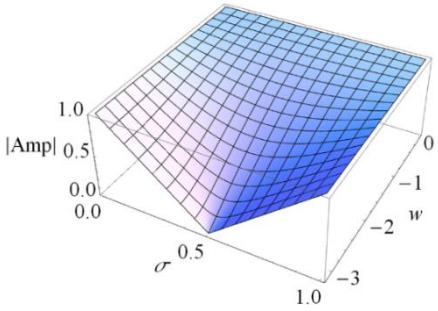

(b) Magnitude of the amplification factor

Figs. 5.1 (a) Amplification factor and (b) its magnitude for the case $K = 1$

For $K = 2$, the P1 (or scheme III), P0I0 (or scheme V), and I1 (or cubic spline) schemes all have the same two eigenvalues or amplification factors. The magnitudes of these two eigenvalues (principal and second) as functions of σ and w are shown in Fig. 5.2.

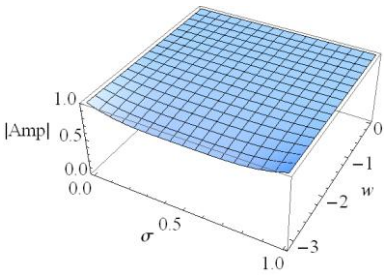

(a) Principal eigenvalue

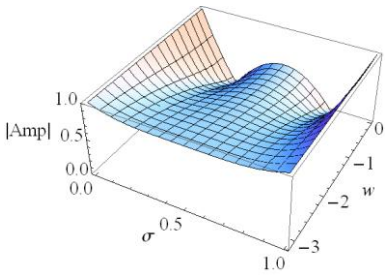

(b) Second (spurious) eigenvalue

Fig. 5.2 Magnitude of the two amplification factors for the case $K = 2$.

For $K = 3$, the P2, P1I0, P0I1, and I2 schemes all have the same sets of eigenvalues whose magnitudes are shown in Fig. 5.3.

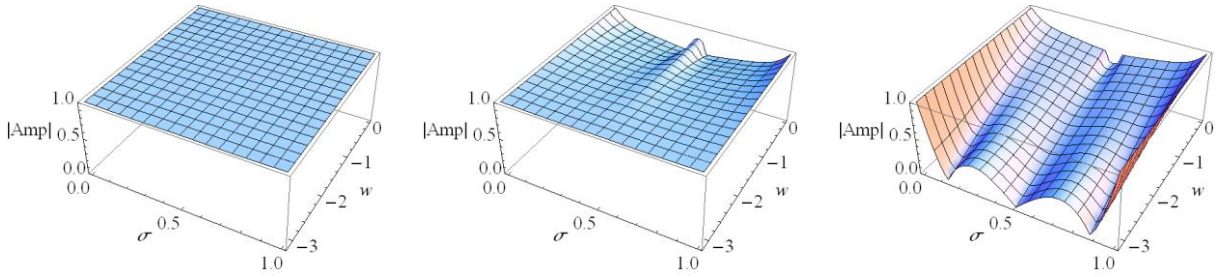

(a) Principal eigenvalue (b) Second eigenvalue (c) Third eigenvalue

Fig. 5.3 Magnitude of the three eigenvalues for the case $K = 3$.

For $K = 4$, the P3, P2I0, P1I1, P0I2, and I3 schemes all have the same sets of eigenvalues whose magnitudes are shown in Fig. 5.4.

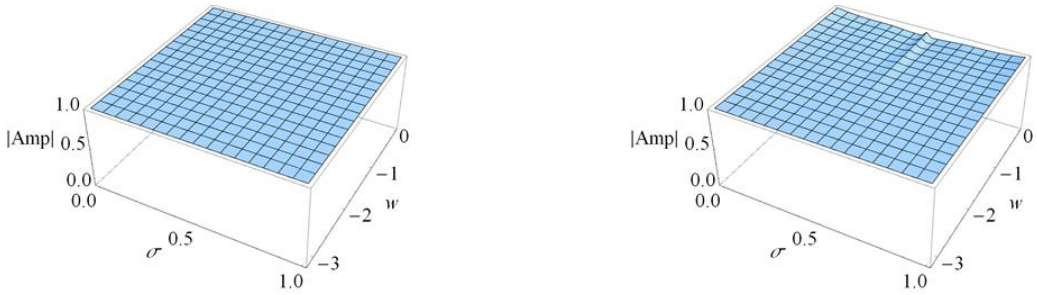

(a) Principal eigenvalue (b) Second eigenvalue

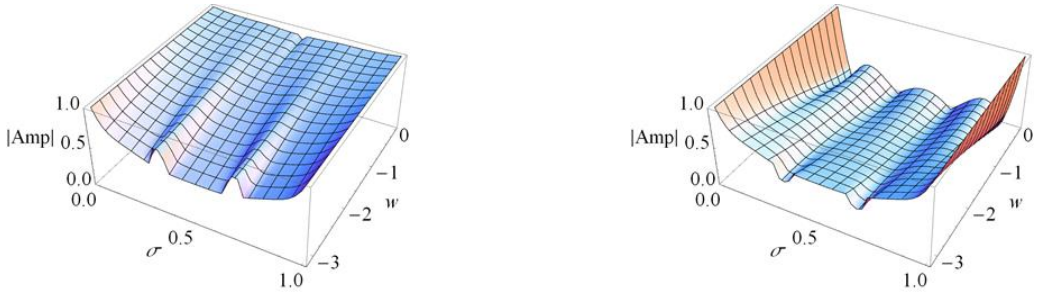

(a) Third eigenvalue (b) Fourth eigenvalue

Fig. 5.4 Magnitude of the four eigenvalues for the case $K = 4$.

Accuracy.

To calculate the order of accuracy, denote the principal eigenvalue of $\boldsymbol{A}$ by $e_p = e_p(\sigma, w)$. This value approximates $e^{-i\sigma w}$. (Advecting one cell width corresponds to the exact multiplication factor of e^{-iw}.) A scheme is accurate to order m if, for a fixed σ, e_p approximates $e^{-i\sigma w}$ to $O(w^{m+1})$ for small w,

$$e_p - e^{-i\sigma w} = O(w^{m+1}). \tag{5.6}$$

In practice, it is difficult if not impossible to derive a Taylor series expression for e_p when $K > 2$. Therefore, we obtain the order of accuracy of a scheme by a numerical calculation as follows. First, set $\sigma = \sigma_0 = 0.8$, say, and $w = w_c = \pi/4$ (subscript 'c' for coarse). We can calculate the coarse mesh error

$$\mathrm{er}_c = e_p(\sigma_0, w_c) - e^{-\boldsymbol{I}\sigma_0 w_c}. \tag{5.7}$$

By halving the wave number, $w_f = w_c/2 = \pi/8$ (equivalent to doubling the number of mesh points), the corresponding fine mesh error is

$$\mathrm{er}_f = e_p(\sigma_0, w_f) - e^{-\boldsymbol{I}\sigma_0 w_f}. \tag{5.8}$$

For a scheme to be *m*-th order accurate, after one time step,

$$\left|\frac{\mathrm{er}_c}{\mathrm{er}_f}\right| \approx 2^{m+1}. \tag{5.9}$$

That is,

$$m \approx \frac{\mathrm{Log}\left(\left|\frac{\mathrm{er}_c}{\mathrm{er}_f}\right|\right)}{\mathrm{Log}(2)} - 1. \tag{5.10}$$

Thus, for a scheme to be of order m, when we march to a certain final time, doubling the mesh results in reducing the error by a factor of 2^m.

For each constant K, the PμIν schemes such that $\mu + \nu = K - 2$ are accurate to order $2K - 1$ as shown in Table 5.1 below. They also have the same K sets of eigenvalues as discussed earlier (Figs. 5.2-5.4).

Table 5.1. Errors and order of accuracy of PμIν schemes with a fixed number of degrees of freedom K. Here, $\sigma = 0.8$, coarse mesh error corresponds to $w_c = \pi/4$, and fine mesh error, $w_f = w_c/2 = \pi/8$.

K	Coarse Mesh Error	Fine Mesh Error	Ord. of Acc.
1	$-4.33 \times 10^{-2} + 2.21 \times 10^{-2} i$	$-1.2 \times 10^{-2} + 2.87 \times 10^{-3} i$	0.98
2	$-4.85 \times 10^{-4} + 4.79 \times 10^{-4} i$	$-4.06 \times 10^{-5} + 1.68 \times 10^{-5} i$	2.96
3	$-2.26 \times 10^{-6} + 2.24 \times 10^{-6} i$	$-4.62 \times 10^{-8} + 1.91 \times 10^{-8} i$	4.99
4	$-7.24 \times 10^{-9} + 5.58 \times 10^{-9} i$	$-3.47 \times 10^{-11} + 1.17 \times 10^{-11} i$	6.96

6 Conclusions and Discussion

In conclusion, high-order methods (third and higher) are currently an important subject of research in CFD. Van Leer's schemes III and V are both third-order accurate, the former is piecewise linear and the latter piecewise parabolic. Here, schemes III and V are shown to be equivalent in the sense that they yield identical (reconstructed) solutions. This equivalence is counter intuitive since it is generally believed that piecewise linear and piecewise parabolic methods cannot produce the same solutions due to their different degrees of approximation. The finding also shows a key connection between the approaches of discontinuous and continuous polynomial approximations. In addition to the discussed equivalence, a framework using both projection and interpolation that extends schemes III and V into a single family of high-order schemes is introduced. For these high-order extensions, it is demonstrated via Fourier analysis that schemes with the same number of degrees of freedom K per cell, in spite of the different polynomial degrees, share the same sets of eigenvalues and thus, have the same stability and accuracy. Moreover, these schemes are accurate to order $2K-1$, which is higher than the expected order of K. The finding that schemes with the same K share the same sets of eigenvalues also points to a possible equivalence relation in a manner similar to the equivalence between schemes III and V. Such an equivalence for the general case, however, has not been found by this author. Finally, extensions of these schemes to the case of multiple dimensions and systems of equations remain to be explored.

Acknowledgments

This work was supported by the Transformational Tools and Technologies Project of NASA. The author wishes to thank Drs. Seth Spiegel and Xiao-Yen Wang for their reviews and suggestions.

References

B. Cockburn, G. Karniadakis, and C.-W. Shu (2000), The development of discontinuous Galerkin methods, Springer, pp 3–50.

P. Colella and P. Woodward (1984), The piecewise parabolic method (PPM) for gas-dynamical simulations, J. Comput. Phys., 54, pp. 174--201.

T.A. Eymann (2012), Active Flux Schemes, Ph.D. Dissertation, University of Michigan.

T.A. Eymann and P.L. Roe (2011), Active Flux Schemes for systems, AIAA paper 2011-3840.

D. Fan and P. L. Roe (2015), Investigations of a New Scheme for Wave Propagation, AIAA paper 2015-2449

S.K. Godunov (1959), A finite difference method for the numerical computation of discontinuous solutions of the equations of fluid dynamics, Mat. Sb., 47, pp. 357-393.

J.S. Hesthaven and Tim Warburton (2008), Nodal Discontinuous Galerkin Methods, Springer.

F.B. Hildebrand (1987), Introduction to Numerical Analysis, Second Edition, Dover Books on Advanced Mathematics.

H.T. Huynh (2006), An upwind moment scheme for conservation laws, Proceedings of the Third International Conference on Computational Fluid Dynamics, ICCFD3, Toronto, Springer, pages 761-766.

H.T. Huynh (2007), A flux reconstruction approach to high-order schemes including discontinuous Galerkin methods, AIAA Paper 2007-4079.

H.T. Huynh (2009), A Reconstruction Approach to High-Order Schemes Including Discontinuous Galerkin for Diffusion, AIAA Paper 2009-403.

H.T. Huynh (2013), High-Order Space-Time Methods for Conservation Laws, AIAA Paper 2013-2432.

H.T. Huynh, Z.J. Wang, and P.E. Vincent (2014), High-order methods for computational fluid dynamics: A brief review of compact differential formulations on unstructured grids, Computers & Fluids, (2014) 98: 209–220

L. Khieu, Y. Suzuki, and B. Van Leer (2009), An Analysis of a Space-Time Discontinuous-Galerkin Method for Moment Equations and Its Solid-Boundary Treatment, AIAA 2009-3874.

Y. Liu, M. Vinokur, Z.J. Wang (2006), Discontinuous spectral difference method for conservation laws on unstructured grids. J Comput. Phys., 216:780–801

M. Lo (2011), A Space-Time Discontinuous Galerkin Method for Navier-Stokes with Recovery, Ph.D. Dissertation, University of Michigan.

W.H. Reed and T.R. Hill (1973), Triangular mesh methods for the neutron transport equation, Los Alamos Scientific Laboratory Report, LA-UR-73-479.

Y. Suzuki (2008), Discontinuous Galerkin Methods for Extended Hydrodynamics, PhD Dissertation, University of Michigan.

Y. Suzuki and B. Van Leer (2007), An analysis of the upwind moment scheme and its extension to systems of nonlinear hyperbolic-relaxation equations, AIAA 2007-4468.

B. Van Leer (1977), Towards the ultimate conservative difference scheme: IV. A new approach to nzmerical convection, J. Comput. Phys., 23, pp. 276-298.

B. Van Leer (1979), Towards the ultimate conservative difference scheme: V. A second-order sequel to Godunov's method, J. Comput. Phys., 32, pp. 101-136.

B. Van Leer and S. Nomura (2005), Discontinuous Galerkin for diffusion, 17th AIAA-CFD Conference, AIAA paper 2005-5108.

Z.J. Wang, L. Zhang, Y. Liu (2004), Spectral (finite) volume method for conservation laws on unstructured grids IV: extension to two-dimensional Euler equations, J Comput. Phys., 194(2):716–41.